Metrol. Meas. Syst., Vol. 29 (2022), No. 2
DOI: 10.24425/mms.2022.140038

METROLOGY AND MEASUREMENT SYSTEMS
Index 330930, ISSN 0860-8229
www.metrology.wat.edu.pl

A NOVEL, MACHINE LEARNING-BASED FEATURE EXTRACTION METHOD FOR DETECTING AND LOCALIZING BEARING COMPONENT DEFECTS

Bilal Djamal Eddine Cherif[1)], Sara Seninete[2)], Mabrouk Defdaf[1)]

1) *Department of Electrical Engineering, Faculty of Technology, University of M'sila, M'sila 28000, Algeria*
(✉ *cherif.bilaldjamaleddine@univ-msila.dz*, +213 663082807, *mabrouk.defdaf@univ-msila.dz*)
2) *Department of Electrical Engineering, Faculty of Technology, University of Mostaganem, Mostaganem 27000, Algeria*
(*sara.seninete@univ-mosta.dz*)

Abstract

Vibration analysis for conditional preventive maintenance is an essential tool for the industry. The vibration signals sensored, collected and analyzed can provide information about the state of an induction motor. Appropriate processing of these vibratory signals leads to define a normal or abnormal state of the whole rotating machinery, or in particular, one of its components. The main objective of this paper is to propose a method for automatic monitoring of bearing components condition of an induction motor. The proposed method is based on two approaches with one based on signal processing using the Hilbert spectral envelope and the other approach uses machine learning based on random forests. The Hilbert spectral envelope allows the extraction of frequency characteristics that are considered as new features entering the classifier. The frequencies chosen as features are determined from a proportional variation of their amplitudes with the variation of the load torque and the fault diameter. Furthermore, a random forest-based classifier can validate the effectiveness of extracted frequency characteristics as novel features to deal with bearing fault detection while automatically locating the faulty component with a classification rate of 99.94%. The results obtained with the proposed method have been validated experimentally using a test rig.

Keywords: Induction motor, bearing, fault, outer race, inner race, ENV, RF.

1. Introduction

Induction motors take an important place in the production industries. Proper dealing with malfunctions of these motors can satisfy the compromise between the production and the maintenance cost. Statistical studies show that most of the faults in induction motors are related to bearings with an occurrence of 40-50%. Predicting rolling component faults dramatically reduces maintenance costs such as motor shutdown and spare parts consumption. The monitoring of bearings is a very important aspect of reliability and safety of operation of induction motors; it is based mainly on the extraction of information revealing the degradation conditions encountered. Several physical quantities were used such as flux, torque, speed, temperature, stator current, oil analysis and vibration analysis to monitor the condition of the bearings [1, 2].

Vibration analysis is the most widely used technique for monitoring and diagnosing bearing faults. Vibration analysis is performed at three levels: supervision, diagnosis and monitoring. Supervision uses the so-called global indicators which characterize the modification of the rolling behavior. Second, the diagnosis is based on signal processing tools in order to locate and identify faults. Then, monitoring, consists in observing the damage status of each of the defective items [3].

Article history: received November 24, 2021; revised February 20, 2022; accepted March 21, 2022; available online April 27, 2022.

Signal processing-based fault diagnosis methods have recently been most commonly used in the field of fault detection. Among these methods, there are two most popular analysis methods, namely, *Power Spectral Density* (PSD) and spectral *Envelope* (ENV), where PSD-based analysis is the best-known [4, 5]. The ENV method uses the high resonant frequency of the bearing to extract the information necessary to determine the presence of the defect and highlights this information in a frequency range normally observed in vibration analysis *i.e.*, $0 \leq f \leq 1500$ Hz [6].

To automate the diagnosis, the localization of the fault after its detection must take place. Machine learning methods offer classification of different faults while ensuring better fault localization. Implementation of machine learning in addition to signal processing leads to automatic fault monitoring [7]. Among the machine learning methods, the following methods are the most widely used: artificial neural network, multi-layer perceptron, naïve-bays, k-nearest neighbors and random forests. In this regard, several researchers have proven the effectiveness of *Random Forests* (RF) giving a high classification rate [8]. RF is composed (as the term "forest" indicates) of a set of binary decision trees in which randomness has been introduced. These trees are distinguished from each other by the subsample of data on which they are trained. These subsamples are drawn at random (hence the term "random") from a dataset [9]. The technique of RF modifies the bagging method applied here to trees by adding a criterion of decorrelation between these trees. The idea behind this method is to reduce the correlation without overly increasing the variance. The principle consists in choosing at random a subset of variables which will be considered at each level of choice as the best node of the tree [10].

Concerning the bearing fault diagnosis, several scientific works have been published for the detection and localization of defects in bearing components.

In [10], the authors propose a novel method for the inter-shaft bearing faults diagnosis using acoustic emission signals. Multiple information entropies are used to serve as features training the RF model. The method is validated with an accuracy of 93.75%. However, the faults are simulated and are not experimentally realized in the bearings. This fact can reduce the effectiveness of the method. Otherwise, acoustic emission signals contain a lot of mechanical noise due to a complicated signal transmission path. Thus, a de-noising method must be used as pre-processing in order to filter and reduce the noise when applying the multi-domain entropy method.

The authors in [11] analyze vibration signals using the fast Fourier transform and the Hilbert transform to obtain the envelope signals. Then, to automate the bearing faults detection process, three types of neural networks were tested and compared in terms of the network architecture and the number of parameters of the learning process. The detector based on the Hilbert Transform increases the stability and has an accuracy varying between 95% and 100%.

A condition monitoring method for detecting different fault severities in the outer race of bearings is proposed in [12]. Different physical magnitudes, notably vibrations and stator current, are represented in both time and frequency domains. In this regard, hybrid features are extracted leading to a high-performance signal characterization. However, a feature reduction technique is necessary used to keep the informative features while reducing the dimensionality. A neural network-based machine learning technique correctly identifies the fault severity in the outer race of a bearing with an accuracy of 98.7%.

In [13], the authors present a literature survey of the works dealing with bearing fault detection from 2012 to 2019. This study indicates the effectiveness of different machine and deep learning techniques in the bearing fault monitoring. Furthermore, a comparative study is carried out between three classification techniques for the bearing fault detection, namely; random forests, an artificial neural network, and an autoencoder. This later gives the highest accuracy of 91% compared to the two other techniques.

In this paper, the proposal of a bearing condition monitoring method is supported by the use of the Hilbert-based signal processing technique. Vibration signals are analyzed in order to avoid the pre-processing step. Statistical frequency-domain features are preferred due to their simplicity of calculation and their significance in fault characterization. In fact, an important aspect related to changes of the load and the fault diameter is proposed for the features extraction which is obtained from the spectral envelope to characterize the acquired vibration signals.

Furthermore, although the analysis of fault-related frequency components produced by bearing failures leads to detecting the faults, additional knowledge and experience is necessary to classify the faults. Random forests-based machine learning is incorporated to achieve automatic fault diagnosis. Thereby, the effectiveness of this proposal is proved since different bearing conditions are effectively diagnosed and identified using the benchmarked dataset provided by *Case Western Reserve University* (CWRU). The assessed conditions comprise a healthy condition and different faulty conditions with a damage of 0.1778 mm and 0.5334 mm for the inner race, outer race and rolling element while the motor drives no-load, then drives three different loads.

The rest of the paper is organized as follows: in Section 2, we briefly discuss the characteristic frequencies of a faulty bearing. The third Section 3 represents the test rig and the data set used in this paper. In the next section, we detail the method of fault detection while localizing the faulty components in a bearing. Section 5 deals with the criteria evaluation of the method of localization of the faulty bearing component. Then, in the next section, we justify the preference of the method using a comparison of the method proposed in this paper with previously completed works in terms of performance. Finally, Section 7 closes the paper with a conclusion.

2. Brief on the frequencies characterizing the bearing faults

The rolling bearing structure is shown in Fig. 1 and the frequencies characterizing the faults are determined from the geometry of the bearing shown in Fig. 2.

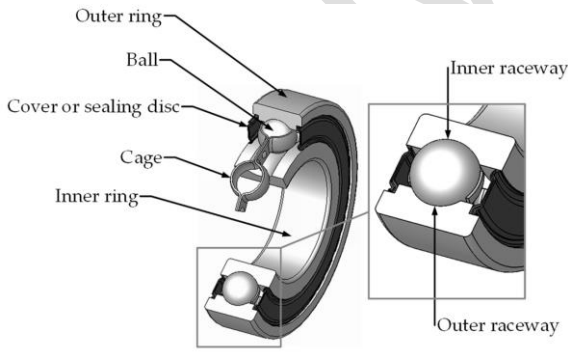

Fig. 1. Diagram of the construction of a rolling bearing [11].

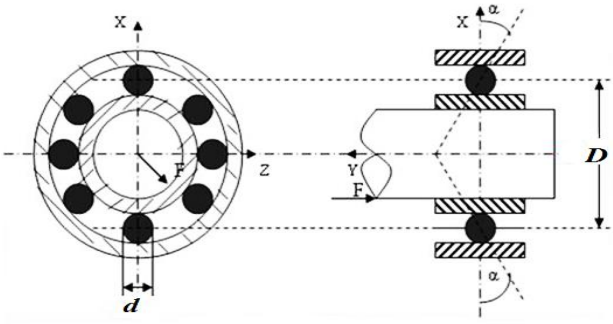

Fig. 2. Geometric characteristic of a bearing.

With n_b - the number of rolling components, D - the intermediate diameter, d - the diameter of the rolling components, α - the contact angle, f_r - the rotation frequency is defined as follows:

$$f_r = \frac{n}{60}, \tag{1}$$

where n is rotation speed of the induction motor.

The vibratory signature of a fault affecting a bearing outer race is a comb of lines whose pitch corresponds to the frequency characterizing the fault in the vibration spectrum. Each component of this comb is associated with a pair of side bands spaced apart by the frequency of rotation. Its characteristic frequency is given by the following equation [14]:

$$f_{or} = \frac{n_b}{2} f_r \left[1 - \frac{d}{D} \cos\alpha \right]. \tag{2}$$

The vibratory signature of a fault affecting the inner race of a bearing is a comb of lines whose pitch corresponds to the frequency characterizing the fault in the vibration spectrum. This frequency is modulated by the frequency of rotation of the shaft (side bands around the fault line). Its characteristic frequency is given by [15]:

$$f_{ir} = \frac{n_b}{2} f_r \left[1 + \frac{d}{D} \cos\alpha \right]. \tag{3}$$

The vibration signature of a defect affecting the rolling element is a comb of lines. Each component of this comb is associated with several pairs of sidebands spaced at the frequency of the cage defined by the equation (4). The characteristic frequency of the rolling element fault is given by the equation (5) [15]:

$$f_C = \frac{f_r}{2} \left(1 \pm \frac{d}{D} \cos\alpha \right), \tag{4}$$

$$f_{re} = \frac{D}{d} f_r \left[1 - \left(\frac{d}{D} \cos\alpha \right)^2 \right] \tag{5}$$

3. Test rig and Data Set

The vibration data sets can be obtained from CWRU [16]. A test rig permits extracting the vibration signals from the bearings, as Fig. 3, shows. The equipment is made up of an electric motor, a torque transducer, a dynamometer, and the tested bearings. An electric motor with a power of 1.5 kW drives a load through a shaft connected by a coupling. On this shaft, a torque transducer and encoder are built-up to ensure speed and torque data measurements. Then, accelerometers are combined with the motor housing with a magnetic base in order to provide the vibration signals.

In order to apply different motor loads (0–12.3Nm), an embedded electronic control unit was used with a dynamometer known as absorbing dynamometer. This latter behaves like a load driven by the induction motor. The amount of the applied torque is proportional to the motor load that has been handled by variable frequency drive using the control unit. Thus, increasing the motor load leads to increasing the torque with simultaneous reduction of shaft speed. The motor load of 0 Nm represents the condition of no-load.

The vibration data sets gather about 20 normal and faulty cases of bearings. Among them, four cases are issued under normal conditions, while the rest of the data sets are collected from faulty bearings with 0.1778 mm minor fault and 0.5334 mm severe fault. The faults addressed herein are those of the inner race, outer race and rolling. Defects in the outer race, ball and inner race are introduced into the bearing by electroerosion (EDM - *Electrical Discharge Machining).* The EDM technique is a process for treating hard metals or mechanical components that could not be penetrated with traditional processes. The defect then corresponds to a circular hole; its

size is thus defined by the diameter. The defect diameter of 0.1778 mm corresponds to an incipient defect and the defect diameter of 0.5334 mm is a deep defect.

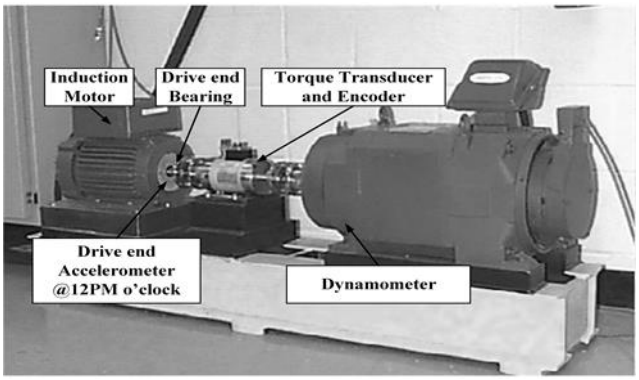

Fig. 3. Experimental test rig.

Experimentally, accelerometers used to measure the data sets are connected to the motor drive end based on a magnetic base. Accelerometers were placed at the 12 o'clock position at both the drive end and the fan end of the motor housing. During some experiments, an accelerometer was attached to the motor supporting base plate as well. Vibration signals were collected using a 16 channel DAT recorder, and were post processed in MATLAB environment. The data sets are sampled at a rate of 12000 samples/s [16]. During each test, the average speed measured represents the provided rotational speed.

4. Bearing Fault Detection and Localization Method

4.1. Fault detection based on the Hilbert envelope analysis

A localized defect in a bearing results in the presence of a periodic pulse in the time signal that can be used for diagnostics. The Hilbert Envelope analysis of is a technique for early detection of shock-type faults. It is based on the Hilbert transform which is widely used for diagnosis of rotating machinery.

The Hilbert transform of a signal $x(t)$ is defined by the following equation [17]:

$$\hat{x}(t) = \frac{1}{\pi}\int\left(\frac{x(\tau)}{t-\tau}\right)dt\,, \tag{6}$$

where $\hat{x}(t)$ is the imaginary part of the analytical signal, $z(t)$ which is defined as follows [18]:

$$z(t) = x(t) + j\,\hat{x}(t) = x(t) + jH\left[x(t)\right] = A(t)e^{j\varphi(t)}, \tag{7}$$

where *H [x (t)]* is the Hilbert transform of *x (t).*

The envelope of signal *A (t)* is represented by the modulus of the analytical signal *A(t)=[x(t)]*. The phase and instantaneous frequency of the signal are given by the following equations [19, 20]:

$$\varphi(t) = arctg\left[\frac{\hat{x}(t)}{x(t)}\right], \tag{8}$$

$$\omega(t) = \frac{d\varphi(t)}{dt}. \tag{9}$$

In practice, the envelope method requires a series of processing of raw time signal before obtaining the result. These steps are summarized as follows:

- ***Step 01:*** Filtering the raw signal to remove unwanted components,
- ***Step 02:*** Applying the Hilbert transform to calculate the envelope,
- ***Step 03:*** Calculating the envelope spectrum, then extracting information about the fault.

Table 1 shows the dimensions and parameters of 6205-2RSJEM-SKF *i.e.*, a typical bearing.

Table 1. Parameters of the bearing 6205-2RSJEM-SKF.

Parameters	Values
Bearing type	6205-2RSJEM-SKF
Inner race diameter	25 mm
Outer race diameter	52 mm
Intermediate diameter	39 mm
Ball diameter	8 mm
Number of balls	9
Contact angle	0 rad

The theoretical fault frequencies used the two equations (1) and (2) for the example of the motor with no-load under fault diameter of 0.1778 mm are summarized in Table 2.

Table 2. Calculated theoretical frequencies.

Rotation frequency	Outer race frequency	Rolling element frequency	Inner race frequency
29.95 Hz	107.12 Hz	139.86 Hz	162.42 Hz

Fig. 4 shows the vibratory signatures and the spectral envelope analysis for the following cases: healthy bearing, bearing with an outer race fault, bearing with a rolling element fault and a bearing with an inner race fault for the example of the motor with no-load under fault diameter of 0.1778 mm. The ENV in Fig. 4 a shows clearly the frequency of rotation f_r = 30 Hz and its harmonic 2 f_r. One can see that there are no frequencies of faults. This confirms that the bearing is in healthy condition. The envelope spectrum of the vibratory signal of the bearing under outer race fault is shown in Fig. 4 b. For the rotation speed of 1797 RPM, the ENV shows the following frequency peaks: f_{or} = 108 Hz, f_{or}-f_r=78 Hz, f_{or} + f_r = 138 Hz, 2f_{or} = 216 Hz, 2f_{or}-f_r = 185 Hz, 3f_{or} = 324 Hz and 3f_{or}-f_r = 293 Hz. These frequencies are very close to those calculated theoretically for the fault of the outer race. Thus, a defect is definitely present in the outer race. When a rolling element fault occurs in bearing, the envelope spectrum of the vibratory signal is as shown in Fig. 4 c represents the following frequency peaks: f_{re} = 140.09 Hz, 3 f_{re} = 420.27 Hz and 4f_{re} = 560.36 Hz. These frequencies are very close to those calculated theoretically for the fault of the rolling element. Accordingly, a defect the rolling element is present. Likewise, Fig. 4 d represents the envelope spectrum of the vibratory signal when the bearing has an inner race fault. Also, for the speed of rotation of 1797 rpm, the following frequency peaks appear: f_{ir} = 162 Hz, f_{ir}-2f_r = 102 Hz, f_{ir} + 2f_r = 222 Hz, 2f_{ir} = 324 Hz and 2f_{ir}+2f_r=384 Hz. These frequencies are very close to those calculated for the fault of the inner race. This clearly indicates the presence of a fault in the inner race.

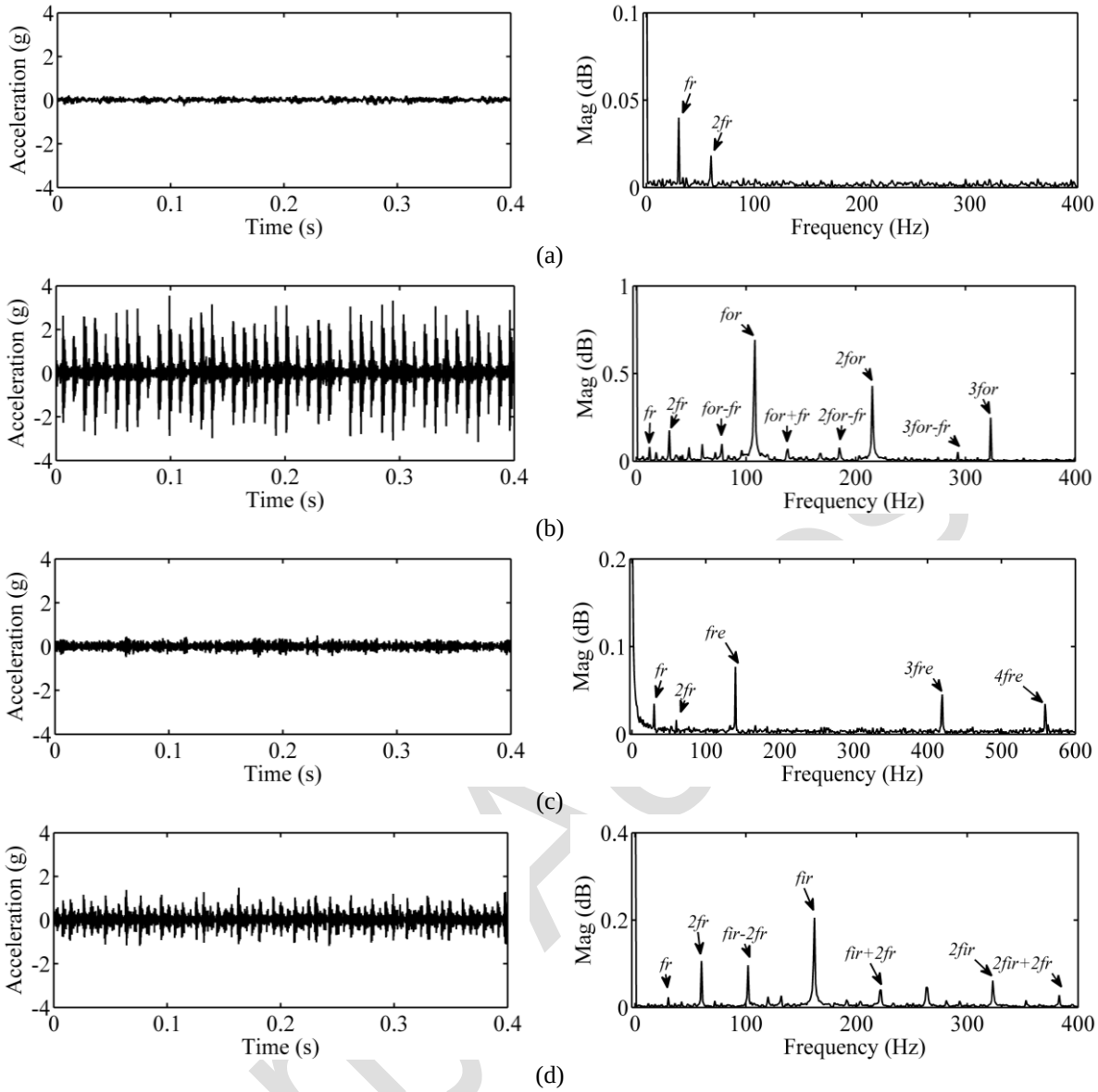

Fig. 4. Vibratory signatures and spectral envelope analysis. (a): healthy bearing. (b): bearing with an outer race fault. (c): bearing with a rolling element fault. (d): bearing with an inner race fault.

4.2. Localization of the defected component based on RF

The RF classification algorithm is given by the following steps [21]:

Step 01: Collect the training sample set and extract features for each sample to form a sample feature set with a total of *N* samples with each sample having *L* feature attributes;

Step 02: Perform independent repeated sampling in the sample feature set *S*, select *n* samples as 1 sample set, repeat *K* times, and obtain *K* sample sets;

Step 03: Randomly select l from all *L* feature attributes in each sample set, and then obtain *K* sample sets with l feature attributes;

Step 04: Take 1 feature attribute as input to the decision tree, so *K* sample sets can generate *K* decision trees to form an RF;

Step 05: Diagnose the test samples with the generated decision tree and use integrated voting calculation to obtain the diagnosis and recognition results of the RF according to the recognition results of all decision trees.

4.3. New feature extraction method

In order to extract the features from the characteristic frequency peaks given by the ENV of the different healthy and faulty cases, the amplitudes of these frequencies are analyzed then for four different loads (0 Nm, 4 Nm, 8 Nm and 12.3 Nm) and under different fault diameters (0 mm, 0.1778 mm, 0.3556 mm and 0.5334 mm). Several instances of amplitudes of selected harmonics are shown in Fig. 5 for the examples of 0 Nm load with varying fault diameter (Fig. 5 a) and the examples of a severe diameter fault while changing the load torque (Fig. 5 b).

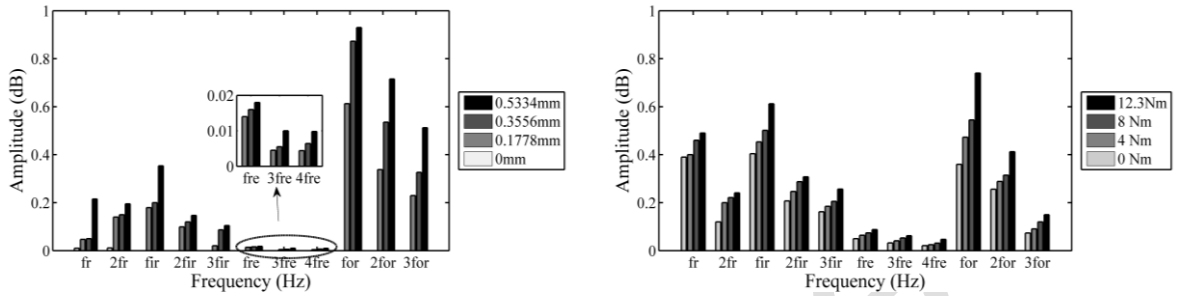

(a) (b)

Fig. 5. Selected harmonic amplitudes of characteristic frequencies obtained using ENV for (a): different fault diameters with no-load. (b): different load torques under 0.5334 mm fault diameter

Detailed analysis allowed checking how the load torque and fault diameter affected the harmonic amplitudes of characteristic frequencies. From Fig. 5, the selected harmonics are characterized by certain accordance with the change in the load torque and fault diameter value. A significant increase in amplitude is observed when the fault diameter increases as shown in Fig. 5 a. Moreover, once the load torque value increases as shown in Fig. 5 b, the selected harmonics are characterized by an increase in amplitude. This condition is fulfilled by the following frequencies: f_r, $2f_r$, f_{ir}, $2f_{ir}$, $3f_{ir}$, f_{re}, $3f_{re}$, $4f_{re}$, f_{or},$2f_{or}$ and $3f_{or}$. This leads to these frequencies being considered as new features that will be used to train the machine learning system based on RF.

4.4. Random forests training system

To complete the diagnosis process for bearing faults, the RF-based machine learning is used to localize the fault (outer race fault, rolling element fault and inner race fault). The structure of the RF model and its schematic diagram are shown in Fig. 6.

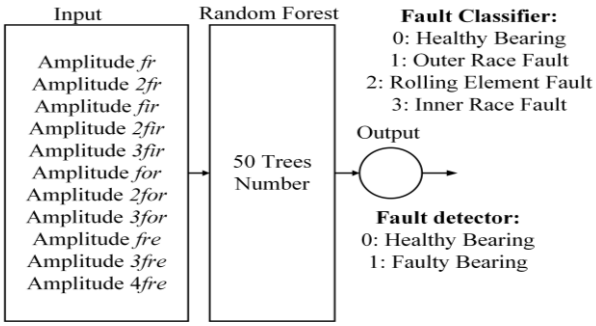

Fig. 6. Schematic diagram of RF.

To train the machine learning technique based on RF, the dataset is divided into a training subset containing 80% (48 signals) of the data and a testing subset containing 20% (12 Signals) of the data. This ratio is selected empirically based on a literature check according to the results in [22], the split ratio 80:20 is observed as a more accurate split when using RF, in particular for bearing fault classification [23].

4.5. Evaluation criteria

The performance of fault classification can be assessed in terms of accuracy, sensitivity, specificity, precision and g-mean.
The accuracy is the percentage of examples that are correctly classified. It is defined as follows [24]:

$$Acc = \frac{T_P + T_N}{T_P + T_N + F_P + F_N}. \tag{10}$$

The sensitivity is the ability to get a positive result when a fault occurs. It is defined as follows [24]:

$$Sens = \frac{T_P}{T_P + F_N}. \tag{11}$$

The specificity is the ability of getting a negative result once the fault is absent. It is defined as follows [24]:

$$Spec = \frac{T_N}{T_N + F_P}. \tag{12}$$

The precision is the ratio of predicted positive examples which are really positive. It is defined as follows [24]:

$$Prec = \frac{T_P}{T_P + F_P}. \tag{13}$$

The G-mean is the geometric mean of sensitivity and precision. It is defined as follows [24]:

$$G - mean = \sqrt{Sens \times Prec}, \tag{14}$$

where T_P: True positive; T_N: True negative; F_P: False positive and F_N: False negative.

Figure 7 shows the accuracy as a function of the trees number. It also shows that 28 is the optimal value for the trees number of RF, with an accuracy equal to 99.94%. From this result it can be concluded that the implementation of RF-based machine learning technique improves the efficiency of localizing the defective bearing component. The difference in the behavior of RF based on the ENV technique can be seen in the result shown in Fig. 7. The output of RF based on ENV gives a good result, as far as the expected output is achieved. This considerably increases the stability and the average accuracy of detection and localization, as shown in Fig. 8.

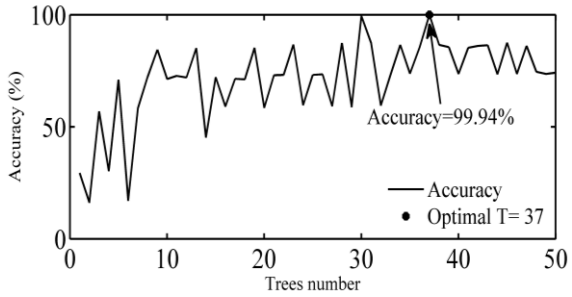

Fig. 7. Accuracy as a function of trees number.

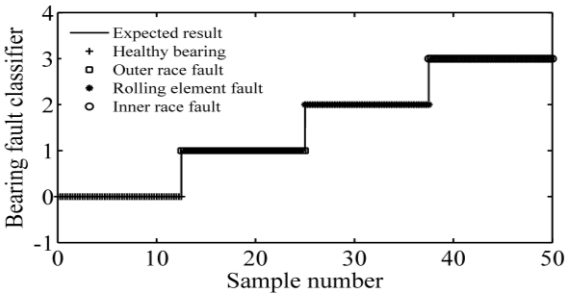

Fig. 8. Waveforms of output values of RF based on ENV.

Table 3 summarizes the evaluation criteria of RF-based machine learning technique.

Table 3. Evaluation criteria of the RF.

Technique	Accuracy	Sensitivity	Specificity	Precision	G-mean
RF	0.9994	0.9870	0.9586	0.9892	0.9881

Although the database is limited, the sensitivity shows a very high rate of 98.70%. This indicates a very high capacity to obtain a true positive result while the bearing is faulty. In addition, the specificity tends towards a very high rate of 95.86%, in other words, the probability of obtaining a negative result when the bearing is healthy, is very common. Moreover, the classifier is very precise with a rate of 98.92%, hence the ability to predict a true positive result from all cases predicted positive by the classifier is very high. Otherwise, the G-Mean rate is an indication of a good or bad performance in the classification of the positive cases even if the negative cases are correctly classified as such. Herein, the G-mean value has a high rate of 98.91% that denotes well classified positive cases. Finally, the accuracy or the rate of correctly classified cases equal is to 99.94%. These performance measurement results prove the classifier's capacities and effectiveness.

5. A Comparison of the Proposed Method with Other Works

A comparison of the method proposed with other recent works, in terms of accuracy, is presented in Table 4.

Table 4. Accuracy comparison among the different methods.

Methods	Classification Accuracy (%)
Linear discriminant analysis - Neural Network [25]	98.7
Multi-domain entropy - RF [10]	94.4
Principal component analysis - long short-term memory - RF [26]	96.04
Multigrained scanning - Cascade forest [27]	96.99-98.54
Genetic algorithm - RF [28]	99.5
ENV - RF	**99,94**

6. Conclusions

In this paper, an automatic diagnosis method for the detection and localization of the outer race fault and inner race fault of bearing of an induction motor is discussed. This proposed diagnosis method using the combination of the Hilbert transform based on the spectral envelope is applied to extract new features for training the random forest-based machine learning. The

Hilbert spectral envelope is used to detect the frequencies that characterize both outer race and inner race faults. Then some frequencies are characterized by certain regularity with the change of the torque value and the fault diameter which leads to extracting new features. The RF machine learning technique shows excellent performance with accuracy equal to 99.94%, in locating defect components in the bearing. The proposed diagnosis method is more efficient and sensitive in detecting and localizing the bearing defect compared with some other recent methods. The various results obtained are validated by several experimental tests carried out at CWRU in order to evaluate the effectiveness of the ENV-RF diagnosis method based on the novel feature extraction method presented in this paper.

RF has several important advantages that should be taken into account, *i.e.*, simpler architecture, shorter learning time and therefore lower computational complexity, including lower requirements on the power of processors during practical implementation. RF still is able to meet these requirements and is much less time-consuming in training and simpler in practical implementation than the more popular deep-learning networks. Also, a further extension of this method is being carried out for other types of induction motor faults.

References

[1] Abdelkader, R., Kaddour, A., Bendiabdellah, A., & Derouiche, Z. (2018). Rolling bearing fault diagnosis based on an improved denoising method using the complete ensemble empirical mode decomposition and the optimized thresholding operation. *IEEE Sensors Journal*, *18*(17), 7166-7172. https://www.doi.org/10.1109/JSEN.2018.2853136.

[2] Chouidira, I., Khodja, D., & Chakroune, S. (2019). Continuous Wavelet Technique for Detection of Broken Bar Faults in Induction Machine. *Traitement du Signal*, *36*(2), 171-176. https://www.doi.org/10.18280/ts.360207. (in French)

[3] Abdelkader, R., Derouiche, Z., Kaddour, A., & Zergoug, M. (2016, November). Rolling bearing faults diagnosis based on empirical mode decomposition: Optimized threshold de-noising method. In *2016 8th International Conference on Modelling, Identification and Control (ICMIC)* (pp. 186-191). IEEE. https://www.doi.org/10.1109/ICMIC.2016.7804296

[4] Brusa, E., Bruzzone, F., Delprete, C., Di Maggio, L. G., & Rosso, C. (2020). Health indicators construction for damage level assessment in bearing diagnostics: A proposal of an energetic approach based on envelope analysis. *Applied Sciences*, *10*(22), 8131. https://www.doi.org/10.3390/app10228131

[5] Eddine, R. C., & Slimane, B. (2020). Detection of bearing defects using Hilbert envelope analysis and fast kurtogram demodulation method. *Journal of Electrical Systems*, *16*(1).

[6] Darji, A. A., Darji, P. H., & Pandya, D. H. (2020). Envelope Spectrum Analysis with Modified EMD for Fault Diagnosis of Rolling Element Bearing. In: Gupta, V., Varde, P., Kankar, P., & Joshi, N. (Eds.), *Reliability and Risk Assessment in Engineering. Lecture Notes in Mechanical Engineering* (pp. 91-99). Springer. https://doi.org/10.1007/978-981-15-3746-2_8

[7] Choudhary, A., Goyal, D., & Letha, S. S. (2020). Infrared thermography-based fault diagnosis of induction motor bearings using machine learning. *IEEE Sensors Journal*, *21*(2), 1727-1734. https://www.doi.org/10.1109/JSEN.2020.3015868

[8] Goyal, D., Dhami, S. S., & Pabla, B. S. (2020). Non-contact fault diagnosis of bearings in machine learning environment. *IEEE Sensors Journal*, *20*(9), 4816-4823. https://www.doi.org/10.1109/JSEN.2020.2964633

[9] Roy, S. S., Dey, S., & Chatterjee, S. (2020). Autocorrelation aided random forest classifier-based bearing fault detection framework. *IEEE Sensors Journal*, *20*(18), 10792-10800. https://www.doi.org/10.1109/JSEN.2020.2995109

[10] Tian, J., Liu, L., Zhang, F., Ai, Y., Wang, R., & Fei, C. (2020). Multi-domain entropy-random forest method for the fusion diagnosis of inter-shaft bearing faults with acoustic emission signals. *Entropy*, *22*(1), 57. https://www.doi.org/10.3390/e22010057

[11] Ewert, P., Orlowska-Kowalska, T., & Jankowska, K. (2021). Effectiveness Analysis of PMSM Motor Rolling Bearing Fault Detectors Based on Vibration Analysis and Shallow Neural Networks. *Energies*, *14*(3), 712. https://www.mdpi.com/1996-1073/14/3/712

[12] Saucedo-Dorantes, J. J., Zamudio-Ramirez, I., Cureno-Osornio, J., Osornio-Rios, R. A., & Antonino-Daviu, J. A. (2021). Condition Monitoring Method for the Detection of Fault Graduality in Outer Race Bearing Based on Vibration-Current Fusion, Statistical Features and Neural Network. *Applied Sciences*, *11*(17), 8033. https://www.doi.org/10.3390/app11178033

[13] Kamat, P., Marni, P., Cardoz, L., Irani, A., Gajula, A., Saha, A., Kumar, S., & Sugandhi, R. (2021). Bearing Fault Detection Using Comparative Analysis of Random Forest, ANN, and Autoencoder Methods. In *Communication and Intelligent Systems* (pp. 157-171). Springer, Singapore. https://www.doi.org/10.1007/978-981-16-1089-9_14

[14] Li, H., Liu, T., Wu, X., & Chen, Q. (2019). Application of EEMD and improved frequency band entropy in bearing fault feature extraction. *ISA Transactions*, *88*, 170-185. https://www.doi.org/10.1016/j.isatra.2018.12.002

[15] Malla, C., & Panigrahi, I. (2019). Review of condition monitoring of rolling element bearing using vibration analysis and other techniques. *Journal of Vibration Engineering & Technologies*, *7*(4), 407-414. https://www.doi.org/10.1007/s42417-019-00119-y

[16] Bearing Data Center - Case Western Reserve university http://csegroups.case.edu/bearingdatacenter/pages/welcome-case-western-reserve-university

[17] Hoseinzadeh, M. S., Khadem, S. E., & Sadooghi, M. S. (2019). Modifying the Hilbert-Huang transform using the nonlinear entropy-based features for early fault detection of ball bearings. *Applied Acoustics*, *150*, 313-324. https://www.doi.org/10.1016/j.apacoust.2019.02.011

[18] Marques, J. A. L., Cortez, P. C., Madeiro, J. P. D. V., Fong, S. J., Schlindwein, F. S., & De Albuquerque, V. H. C. (2019). Automatic cardiotocography diagnostic system based on Hilbert transform and adaptive threshold technique. *IEEE Access*, *7*, 73085-73094. https://www.doi.org/10.1109/ACCESS.2018.2877933

[19] Guo, M. F., Yang, N. C., & Chen, W. F. (2019). Deep-learning-based fault classification using Hilbert–Huang transform and convolutional neural network in power distribution systems. *IEEE Sensors Journal*, *19*(16), 6905-6913. https://www.doi.org/10.1109/JSEN.2019.2913006

[20] Cherif, B. D. E., Bendiabdellah, A., & Tabbakh, M. (2020). An Automatic Diagnosis of an Inverter IGBT Open-Circuit Fault Based on HHT-ANN. *Electric Power Components and Systems*, *48*(6-7), 589-602. https://www.doi.org/10.1080/15325008.2020.1793835

[21] Liu, P., Zhang, Y., Wu, H., & Fu, T. (2020). Optimization of Edge-PLC-Based Fault Diagnosis with Random Forest in Industrial Internet of Things. *IEEE Internet of Things Journal*, *7*(10), 9664-9674. https://www.doi.org/10.1109/JIOT.2020.2994200

[22] Patgiri R., Katari H., Kumar R., Sharma D. (2019, January) Empirical Study on Malicious URL Detection Using Machine Learning. In: Fahrnberger G., Gopinathan S., & Parida L. (Eds.). *Distributed Computing and Internet Technology. ICDCIT 2019. Lecture Notes in Computer Science*, vol. 11319. Springer, Cham. https://doi.org/10.1007/978-3-030-05366-6_31

[23] Nishat Toma, R., & Kim, J. M. (2020). Bearing fault classification of induction motors using discrete wavelet transform and ensemble machine learning algorithms. *Applied Sciences*, *10*(15), 5251. https://doi.org/10.3390/app10155251

[24] Costache, R., Pham, Q. B., Sharifi, E., Linh, N. T. T., Abba, S. I., Vojtek, M., Vojteková, J., Nhi, P. T. T., & Khoi, D. N. (2020). Flash-flood susceptibility assessment using multi-criteria decision making and machine learning supported by remote sensing and GIS techniques. *Remote Sensing*, *12*(1), 106. https://www.doi.org/10.3390/rs12010106

[25] Saucedo-Dorantes, J. J., Zamudio-Ramirez, I., Cureno-Osornio, J., Osornio-Rios, R. A., & Antonino-Daviu, J. A. (2021). Condition Monitoring Method for the Detection of Fault Graduality in Outer Race Bearing Based on Vibration-Current Fusion, Statistical Features and Neural Network. *Applied Sciences*, *11*(17), 8033. https://www.doi.org/10.3390/app11178033

[26] Zhou, H., Cheng, L., Teng, L., & Sun, H. (2021, May). Bearing Fault Diagnosis Based on RF-PCA-LSTM Model. In *2021 2nd Information Communication Technologies Conference (ICTC)* (pp. 278-282). IEEE. https://www.doi.org/10.1109/ICTC51749.2021.9441578

[27] Qin, X., Xu, D., Dong, X., Cui, X., & Zhang, S. (2021). The Fault Diagnosis of Rolling Bearing Based on Improved Deep Forest. *Shock and Vibration*. https://www.doi.org/10.1155/2021/9933137

[28] Toma, R. N., Prosvirin, A. E., & Kim, J. M. (2020). Bearing fault diagnosis of induction motors using a genetic algorithm and machine learning classifiers. *Sensors*, *20*(7), 1884. https://www.doi.org/10.3390/s20071884

Bilal Djamal Eddine Cherif received his B.Sc. degree in Engineering from the University of M'sila, Algeria in 2010, his M.SC. Degree, and his Ph.D. degree in Electrical Engineering from the University of Sciences and Technology of Oran (USTO-MB), Algeria in 2015 and 2019 respectively. He is currently a Professor Lecturer and researcher at the Electrical Engineering Department, Faculty of Technology at the University of M'sila Algeria. His research interests include electrical machine and drive modeling and analysis, electrical machine and drive control and converters as well as electrical machine and drive fault diagnosis and tolerance and machine learning.

Sara Seninete received her B.Sc. degree in Electrical Engineering in 2014, her M.Sc. in Industrial Computing and Embedded Systems in 2016, and her Ph.D. degree in Signals, Systems Concepts and their Applications in 2021, all from the University of Mostaganem, Algeria. Her research interests include signal processing, machine learning, electrical machine and drive modeling and analysis, electrical machine and drive control and converters as well as electrical machine and drive faults diagnosis and tolerance.

Mabrouk Defdaf received his B.Sc., M.Sc. and Ph.D. degrees in Electromechanical Engineering from Badji-Mokhtar Annaba University Algeria in 2000, 2007 and 2018 respectively. He is a lecturer senior at the University of M'sila in Algeria. His research interests include electrical machine and drive modeling and analysis, electrical machine and drive control and converters as well as electrical machine and drive fault diagnosis and tolerance.